Measurement of the fraction of jet longitudinal momentum carried by Λ_c^+ baryons in pp collisions

S. Acharya *et al.*[*]

(ALICE Collaboration)

Recent measurements of charm-baryon production in hadronic collisions have questioned the universality of charm-quark fragmentation across different collision systems. In this work the fragmentation of charm quarks into charm baryons is probed, by presenting the first measurement of the longitudinal jet momentum fraction carried by Λ_c^+ baryons, $z_\parallel^{\mathrm{ch}}$, in hadronic collisions. The results are obtained in proton-proton (pp) collisions at $\sqrt{s} = 13$ TeV at the LHC, with Λ_c^+ baryons and charged (track-based) jets reconstructed in the transverse momentum intervals of $3 \le p_T^{\Lambda_c^+} < 15$ GeV/c and $7 \le p_T^{\mathrm{jet\ ch}} < 15$ GeV/c, respectively. The $z_\parallel^{\mathrm{ch}}$ distribution is compared to a measurement of D^0-tagged charged jets in pp collisions as well as to PYTHIA 8 simulations. The data hints that the fragmentation of charm quarks into charm baryons is softer with respect to charm mesons, in the measured kinematic interval, as predicted by hadronization models which include color correlations beyond leading-color in the string formation.

Heavy-flavor hadrons are produced in high-energy particle collisions through the fragmentation of heavy (charm and beauty) quarks, which typically originate in hard scattering processes in the early stages of the collisions. The most common theoretical approach to describe heavy-flavor production in hadronic collisions is based on the quantum chromodynamics (QCD) factorization approach [1], and consists of a convolution of three independent terms; the parton distribution functions of the incoming hadrons, the cross sections of the partonic scattering producing the heavy quarks, and the fragmentation functions that parametrize the evolution of a heavy quark into given species of heavy-flavor hadrons. As the transition of quarks to hadrons cannot be described in perturbation theory, the fragmentation functions cannot be calculated and must be extracted from data.

Fragmentation functions of charm quarks to charm baryons and mesons have been constrained in e^+e^- [2–4] and e^-p [5,6] collisions, using a variety of different observables, such as the hadron momentum as a fraction of its maximum possible momentum, as dictated by the center-of-mass energy of the collision. Another method to probe the fragmentation of quarks to hadrons is to parametrize the hadron momentum in relation to the momentum of jets, which are collimated bunches of hadrons

giving experimental access to the properties of the scattered quark. Recently, the production of charm mesons in jets, probed via the fractional longitudinal momentum of the jet carried by the D meson, was measured in pp collisions at the Large Hadron Collider (LHC) [7–9] and appears consistent with Monte Carlo (MC) simulations tuned on e^+e^- data. These measurements support the assumption of fragmentation universality across collision systems in the charm-meson sector. This assumption underpins theoretical calculations describing the production of heavy-flavor hadrons in hadronic collisions, which make use of fragmentation functions tuned on e^+e^- and e^-p data.

Measurements of the production cross sections of baryons in pp collisions have questioned the hypothesis of fragmentation universality across collision systems [10]. In the charm sector, which provides a clean probe of hadronization phenomena due to the large mass of the charm quark, recent measurements performed by the ALICE Collaboration [11–19] in pp collisions have shown that the ratio of the Λ_c^+ (and other charm baryons) and D^0 production cross sections measured at low p_T ($\lesssim 12$ GeV/c) is significantly larger than the value expected from MC simulations in which the charm fragmentation is tuned on e^+e^- and e^-p measurements, such as PYTHIA 8 [20] with the Monash tune [21] or Herwig 7 [22]. A recent measurement of the Λ_c^+/D^0 ratio in pp collisions, performed by the ALICE Collaboration in intervals of charged-particle multiplicity, also points to a substantial increase of the Λ_c^+/D^0 ratio with increasing multiplicity, with respect to e^+e^- collisions, starting at very low multiplicities [15].

---

[*]Full author list given at the end of the article.

The study of charm-baryon production in jets can provide more differential insights into hadronization mechanisms in pp collisions, compared to p_T-differential cross sections and yield ratios of heavy-flavor hadrons, allowing for a more accurate study of the dynamical properties of baryon production. In this paper, the first measurement of the longitudinal momentum fraction of the jet carried by Λ_c^+ baryons, $z_\parallel^{\mathrm{ch}}$, is presented. The measurement is performed in pp collisions at $\sqrt{s} = 13$ TeV in the interval $0.4 \leq z_\parallel^{\mathrm{ch}} \leq 1.0$. The $z_\parallel^{\mathrm{ch}}$ distribution, fully corrected to particle level, is presented for prompt (charm-quark initiated) Λ_c^+-tagged jets with $7 \leq p_T^{\mathrm{jet\ ch}} < 15$ GeV/c and $3 \leq p_T^{\Lambda_c^+} < 15$ GeV/c. The results are then compared to PYTHIA 8 simulations [20,23], including a version where mechanisms beyond the leading-color approximation are considered in string formation processes during hadronization [21], and to an analogous measurement of the $z_\parallel^{\mathrm{ch}}$ distribution of D^0 mesons, performed by the ALICE Collaboration [7].

A full description of the ALICE setup and apparatus can be found in Refs. [24,25]. The main detectors used in this analysis are the Inner Tracking System (ITS), which is used for vertex reconstruction and tracking; the Time Projection Chamber (TPC), which is used for tracking and particle identification (PID); and the Time-Of-Flight (TOF) detector, which is used for PID. These detectors cover a pseudorapidity interval of $|\eta| < 0.9$. The analysis was performed on pp collisions at $\sqrt{s} = 13$ TeV, collected using a minimum-bias (MB) trigger during the years 2016, 2017, and 2018. The trigger condition required coincident signals in the two scintillator arrays of the V0 detector, with background events originating from beam-gas interactions removed offline using timing information from the V0. To mitigate against pileup effects, events with multiple reconstructed primary vertices were rejected. To ensure uniform acceptance, only events with a primary-vertex position along the beam axis direction of $|z_{\mathrm{vtx}}| < 10$ cm around the nominal interaction point were accepted. After the selections described above, the data sample consisted of 1.7×10^9 events, corresponding to an integrated luminosity of $\mathcal{L}_{\mathrm{int}} = 29$ nb^{-1} [26].

The Λ_c^+ candidates and their charge conjugates were reconstructed via the hadronic $\Lambda_c^+ \to p K_S^0 \to p \pi^+ \pi^-$ decay channel with a total branching ratio of $(1.10 \pm 0.06)\%$ [27], in the Λ_c^+ transverse-momentum interval of $3 \leq p_T^{\Lambda_c^+} < 15$ GeV/c. Only tracks with $|\eta| < 0.8$ and $p_T > 0.4$ GeV/c, which fulfilled the track quality selections described in Ref. [14], were considered for the Λ_c^+ reconstruction. The Λ_c^+ candidates themselves were reconstructed in the $|y^{\Lambda_c^+}| < 0.8$ rapidity interval. The Λ_c^+-candidate selection was performed using a multivariate technique based on the boosted decision tree (BDT) algorithm provided by the XGBoost package [28].

The features considered in the optimization include the PID signal for the proton track, the invariant mass of the K_S^0-meson candidate, and topological variables that exploit the kinematic properties of the displaced K_S^0-meson decay vertex. The training was performed in intervals of Λ_c^+-candidate p_T, considering prompt signal candidates from PYTHIA 8 events with the Monash tune [20,21], transported through a realistic description of the detector geometry and material budget using Geant 3 [29]. Background candidates were extracted from the sidebands of the invariant-mass distributions in data. The probability thresholds of the BDT selections were tuned, using MC simulations, to maximise the statistical significance for the signal. Further details on the Λ_c^+-candidate reconstruction and machine learning procedure are provided in Ref. [15], where the same reconstruction and BDT model were employed.

For the events where at least one selected Λ_c^+ candidate was identified, a jet-finding procedure was performed, using the FastJet package [30]. Prior to jet clustering, the Λ_c^+-candidate daughter tracks were replaced by the reconstructed Λ_c^+-candidate four-momentum vector. Charged jet finding was carried out on charged tracks with $|\eta| < 0.9$ and $p_T > 0.15$ GeV/c, using the anti-k_T algorithm [31], with a resolution parameter of $R = 0.4$. Tracks were combined using the E-scheme recombination [32], with the jet transverse momentum limited to the interval of $5 \leq p_T^{\mathrm{jet\ ch}} < 35$ GeV/c. The full jet cone was required to be within the ALICE central barrel acceptance, limiting the jet axis to the interval $|\eta_{\mathrm{jet}}| < 0.5$. Only jets tagged via the presence of a reconstructed Λ_c^+ candidate amongst their constituents were considered for the analysis. For events where more than one Λ_c^+ candidate was found, the jet finding and tagging pass was performed independently for each candidate, with only the daughters of that particular candidate replaced by the corresponding Λ_c^+ four-vector each time. In mechanisms of hadronization that include color correlations beyond the leading-color approximation [21], which have been shown to be relevant in hadronic collisions at LHC energies [10], hadrons can be formed in processes that combine quarks from the parton shower with those from the underlying event [33]. As such, the underlying event is not well defined with respect to the measured hadron distributions. Therefore, no underlying event correction is implemented in this work.

The fragmentation of charm quarks to Λ_c^+ baryons is probed by measuring the fraction of the jet momentum carried by the Λ_c^+ along the direction of the jet axis, $z_\parallel^{\mathrm{ch}}$. This is calculated for each jet using

$$z_\parallel^{\mathrm{ch}} = \frac{\boldsymbol{p}_{\mathrm{jet}} \cdot \boldsymbol{p}_{\Lambda_c^+}}{\boldsymbol{p}_{\mathrm{jet}} \cdot \boldsymbol{p}_{\mathrm{jet}}}, \tag{1}$$

where $\boldsymbol{p}_{\mathrm{jet}}$ and $\boldsymbol{p}_{\Lambda_c^+}$ are the jet and Λ_c^+ three-momentum vectors, respectively.

The $z_\parallel^{\mathrm{ch}}$ distributions of true Λ_c^+-tagged charged jets were extracted in intervals of Λ_c^+ p_T and $p_T^{\mathrm{jet\ ch}}$ using a sideband subtraction procedure. To enact this subtraction, the invariant-mass (m_{inv}) distributions of Λ_c^+ candidates, obtained for each Λ_c^+ p_T and $p_T^{\mathrm{jet\ ch}}$ interval, were fitted with a function comprising a Gaussian for the signal and an exponential for the background. The fit parameters were then used to define signal (containing the majority of true signal candidates) and sideband (entirely composed of background candidates) regions, defined by $|m_{\mathrm{inv}} - \mu_{\mathrm{fit}}| < 2\sigma_{\mathrm{fit}}$ and $4\sigma_{\mathrm{fit}} < |m_{\mathrm{inv}} - \mu_{\mathrm{fit}}| < 9\sigma_{\mathrm{fit}}$, respectively, where μ_{fit} and σ_{fit} represent the mean and sigma of the fitted Gaussian distributions. The $z_\parallel^{\mathrm{ch}}(p_T^{\Lambda_c^+}, p_T^{\mathrm{jet\ ch}})$ distributions were extracted in the signal and sideband regions, with the sideband distribution scaled by the ratio of the background function integrals in the signal and sideband regions. The sideband distribution was then subtracted from the signal one, with the resulting distribution scaled to account for the fact that the $2\sigma_{\mathrm{fit}}$ width of the signal region only encompasses approximately 95% of the total signal, to obtain the sideband subtracted $z_\parallel^{\mathrm{ch}}$ yield in each $p_T^{\Lambda_c^+}$ and $p_T^{\mathrm{jet\ ch}}$ interval.

To account for the reconstruction and selection efficiency of the Λ_c^+-tagged jet signal, the sideband subtracted $z_\parallel^{\mathrm{ch}}$ distributions in each $p_T^{\Lambda_c^+}$ and $p_T^{\mathrm{jet\ ch}}$ interval, $N(z_\parallel^{\mathrm{ch}}, p_T^{\Lambda_c^+}, p_T^{\mathrm{jet\ ch}})$, were scaled by the reconstruction efficiency of prompt Λ_c^+-tagged jets, $\epsilon_{\mathrm{prompt}}$, and summed over the entire $p_T^{\Lambda_c^+}$ interval to obtain the efficiency-corrected $z_\parallel^{\mathrm{ch}}$ yield of Λ_c^+-tagged jets, $N^{\mathrm{corr}}(z_\parallel^{\mathrm{ch}}, p_T^{\mathrm{jet\ ch}})$, given by

$$N^{\mathrm{corr}}(z_\parallel^{\mathrm{ch}}, p_T^{\mathrm{jet\ ch}}) = \sum_{p_T^{\Lambda_c^+}} \frac{N(z_\parallel^{\mathrm{ch}}, p_T^{\Lambda_c^+}, p_T^{\mathrm{jet\ ch}})}{\epsilon_{\mathrm{prompt}}(p_T^{\Lambda_c^+})}. \qquad (2)$$

The $\epsilon_{\mathrm{prompt}}(p_T^{\Lambda_c^+})$ efficiency is strongly dependent on $p_T^{\Lambda_c^+}$, ranging from about 20% at $3 < p_T^{\Lambda_c^+} < 4$ GeV/c to 40% at $12 < p_T^{\Lambda_c^+} < 24$ GeV/c, and was calculated using PYTHIA 8 simulations with the Monash tune containing prompt Λ_c^+-tagged jets, transported through the detector using Geant 3. This efficiency does not exhibit a $p_T^{\mathrm{jet\ ch}}$ dependence.

In order to isolate the $N^{\mathrm{corr}}(z_\parallel^{\mathrm{ch}}, p_T^{\mathrm{jet\ ch}})$ distribution of prompt Λ_c^+-tagged jets, a feed-down subtraction was employed to remove the nonprompt (beauty-quark initiated) contribution. The nonprompt cross section was obtained from particle level POWHEG [34] + PYTHIA 6 [35] + EvtGen [36] simulations, as a function of $p_T^{\mathrm{jet\ ch}}$, $p_T^{\Lambda_c^+}$, and $z_\parallel^{\mathrm{ch}}$, and was scaled according to the integrated luminosity of the analyzed data sample and the branching

ratio of the $\Lambda_c^+ \to pK_S^0 \to p\pi^+\pi^-$ decay channel. The resulting particle-level yield was multiplied by the ratio of the nonprompt to prompt Λ_c^+-tagged jet reconstruction and selection efficiency in intervals of $p_T^{\Lambda_c^+}$ and integrated over the $p_T^{\Lambda_c^+}$ range. The simulated nonprompt results were then folded to reconstructed level, using a four-dimensional response matrix generated using nonprompt Λ_c^+-tagged jets in PYTHIA 8 with the Monash tune, transported through a simulation of the ALICE detector using Geant 3. The response matrix was constructed as a function of $p_T^{\mathrm{jet\ ch}}$ and $z_\parallel^{\mathrm{ch}}$ at generator and reconstruction levels. The folded results were then subtracted from the measured $N^{\mathrm{corr}}(z_\parallel^{\mathrm{ch}}, p_T^{\mathrm{jet\ ch}})$ distribution in data, removing the nonprompt contribution. The estimated fraction of Λ_c^+-tagged jets coming from b-quark fragmentation is found to be about 5%, with no significant $z_\parallel^{\mathrm{ch}}$ dependence.

A two-dimensional Bayesian unfolding procedure [37] was performed to correct for detector effects and obtain the $z_\parallel^{\mathrm{ch}}$ distribution for prompt Λ_c^+-tagged jets at particle level. A four-dimensional response matrix as a function of $p_T^{\mathrm{jet\ ch}}$ and $z_\parallel^{\mathrm{ch}}$, at generator and reconstruction levels, was populated with prompt Λ_c^+-tagged jets, obtained with PYTHIA 8 simulations with the Monash tune, passed through a simulation of the ALICE detector using Geant 3. The measured data and response matrix were provided in the intervals of $5 \leq p_T^{\mathrm{jet\ ch}} < 35$ GeV/c and $0.4 \leq z_\parallel^{\mathrm{ch}} \leq 1.0$, with the final unfolded results reported in the intervals $7 \leq p_T^{\mathrm{jet\ ch}} < 15$ GeV/c and $0.4 \leq z_\parallel^{\mathrm{ch}} \leq 1.0$. The extended $p_T^{\mathrm{jet\ ch}}$ range includes two padding intervals for the unfolding from $5 \leq p_T^{\mathrm{jet\ ch}} < 7$ GeV/c and $15 \leq p_T^{\mathrm{jet\ ch}} < 35$ GeV/c, which allow the unfolding to account for migrations in and out of the reported $7 \leq p_T^{\mathrm{jet\ ch}} < 15$ GeV/c interval. Corrections accounting for migrating entries in and out of the response matrix ranges, as modeled by the same MC simulation, were also applied. The corrected $z_\parallel^{\mathrm{ch}}$ distribution is normalized to the total number of Λ_c^+-tagged jets in the reported $z_\parallel^{\mathrm{ch}}$ and $p_T^{\mathrm{jet\ ch}}$ interval.

The systematic uncertainties affecting the measurement were evaluated, in each $z_\parallel^{\mathrm{ch}}$ interval, by modifying the strategy adopted at various steps of the analysis procedure and assessing the impact on the unfolded $z_\parallel^{\mathrm{ch}}$ distribution. The total systematic uncertainty includes contributions from multiple sources. The first considered source is the sideband subtraction procedure, whose contribution (ranging from 3.7% to 7.6% depending on the $z_\parallel^{\mathrm{ch}}$ interval) was estimated by varying the invariant-mass fit parameters as well as the invariant-mass intervals of the signal and sideband regions. The contribution from the BDT selection of Λ_c^+ candidates (from 7.3% to 19%) was estimated by

varying the BDT probability thresholds to induce a 25% variation in the Λ_c^+-tagged jet reconstruction and selection efficiency. The uncertainty from the jet energy resolution (from 4.5% to 19%) was estimated by recalculating the response matrix used for unfolding with a 4% reduced tracking efficiency. The reduction in the tracking efficiency was evaluated by varying the track-selection criteria and propagating the ITS-TPC track-matching efficiency uncertainty. The uncertainty on the feed-down subtraction ($< 2\%$) was estimated by varying the choice of POWHEG parameters considered to generate the feed-down cross section, including the factorization and renormalization scales, as well as the mass of the beauty quark, which were varied according to theoretical prescriptions [38]. Finally the contribution from the unfolding procedure (from 1.1% to 2.7%) was estimated by altering the choice of prior, regularization parameter, and ranges of the response matrix. For each of the aforementioned categories, several variations were made and the root-mean-square of the resulting distributions was considered. The exceptions are related to the contribution associated to the choice of parameters of the POWHEG calculations, where only the largest deviation from the central result, in each direction, was considered, as well as the uncertainty on the jet energy resolution where the variation with respect to the central result was taken as the uncertainty. All uncertainties (other than from the feed-down subtraction) were then symmetrized. The uncertainties were combined in quadrature to obtain

the total systematic uncertainty on the measurement, which ranges from 13% to 28%.

The fully corrected $z_\parallel^{ch}$ distribution of prompt Λ_c^+-tagged charged jets in the intervals of $7 \leq p_T^{jet\ ch} < 15\ \mathrm{GeV}/c$ and $3 \leq p_T^{\Lambda_c^+} < 15\ \mathrm{GeV}/c$ is presented in the left-hand panel of Fig. 1 and compared to PYTHIA 8 simulations with two different tunes. In PYTHIA 8 the Lund string model of fragmentation is employed, where endpoints are confined by linear potentials encoded in strings. For the case of heavy quarks, the Lund fragmentation function is modified to account for the slower propagation of the massive endpoints compared to their massless counterparts. The Monash tune (red-dotted line) [16], in which the charm fragmentation is tuned on e^+e^- measurements, predicts a harder fragmentation than the measurement. An evaluation of the χ^2/ndf between the measured data points and the model was performed, combining the statistical and systematic uncertainties on the data in quadrature and assuming the uncertainties are uncorrelated across the $z_\parallel^{ch}$ intervals. This exercise determines that there is a 0.4% probability that the model describes the data. A better agreement is achieved by PYTHIA 8 with the CR-BLC Mode 2 tune, which includes color reconnection mechanisms beyond the leading-color approximation [23] (green-dashed line). In this model, the minimization of the string potential is implemented considering the SU(3) multiplet structure of QCD in a more realistic way than in the
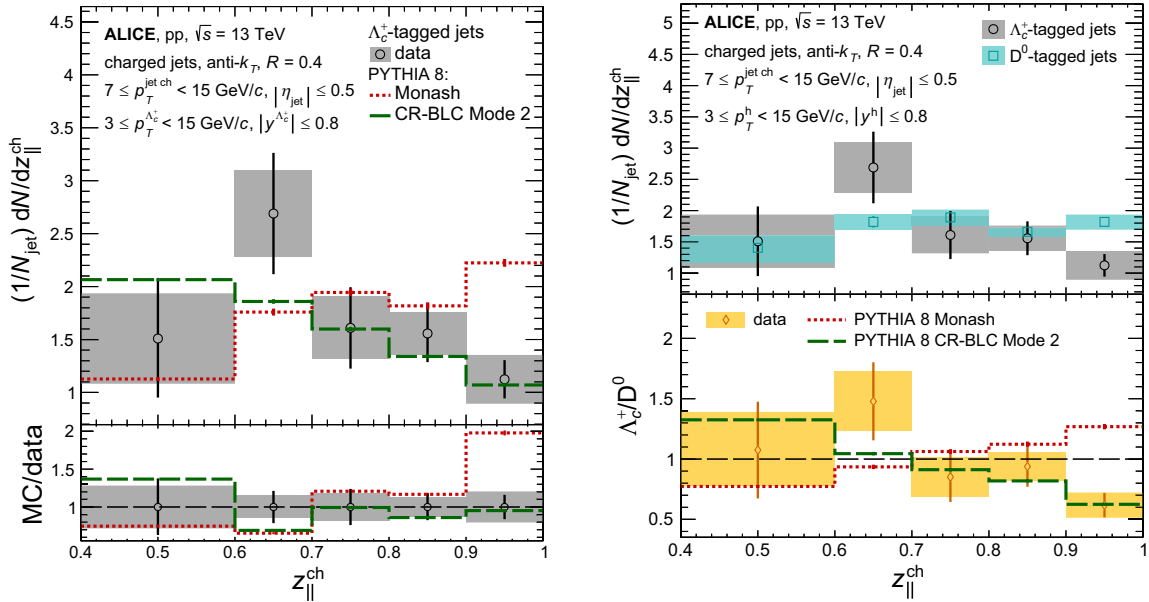

FIG. 1. Left: fully corrected normalized $z_\parallel^{ch}$ distribution of Λ_c^+-tagged charged jets (black open circles) measured in the $7 \leq p_T^{jet\ ch} < 15\ \mathrm{GeV}/c$ and $3 \leq p_T^{\Lambda_c^+} < 15\ \mathrm{GeV}/c$ intervals in pp collisions at $\sqrt{s} = 13$ TeV, compared with predictions from different PYTHIA 8 tunes [20,21,23] (red-dotted and green-dashed lines). The ratios of the MC simulations to the data are shown in the bottom panel. Right: comparison of the measured $z_\parallel^{ch}$ distribution of Λ_c^+-tagged jets and the previously measured $z_\parallel^{ch}$ distribution of D^0-tagged jets [7], obtained in the same kinematic interval. The ratio of the $z_\parallel^{ch}$ distribution of Λ_c^+-tagged and D^0-tagged jets is shown in the bottom panel for both the data and the different PYTHIA tunes.

leading-color approximation, allowing for the formation of "baryonic" configurations where for example two colors can combine coherently to form an anticolor. The same χ^2/ndf approach results in a 78% probability that the model describes the data. The simulation with PYTHIA 8 with the CR-BLC Mode 2 tune also provides a much more accurate description of the Λ_c^+/D^0 cross section ratio, previously measured in pp collisions at the LHC [11–15,39].

In the right-hand panel of Fig. 1, a comparison of the $z_\parallel^{\text{ch}}$ distribution of Λ_c^+-tagged jets and the $z_\parallel^{\text{ch}}$ distribution previously measured for D^0-tagged jets [7] is presented. The latter is consistent with PYTHIA 8 simulations using both the Monash and CR-BLC Mode 2 tunes. The ratio of the two distributions is also presented in the bottom panel. The uncertainty from the jet-energy resolution was considered to be correlated between the Λ_c^+-tagged jet and D^0-tagged jet measurements and was evaluated directly on the ratio of the distributions. The remaining uncertainties were considered uncorrelated when taking the ratio and were then combined in quadrature with the uncertainty of the jet-energy resolution. The uncertainties were considered uncorrelated across the $z_\parallel^{\text{ch}}$ intervals. The same χ^2/ndf exercise described above determines that there is a 12% probability that the measured ratio is described by a flat distribution at unity, hinting at a softer fragmentation of charm quarks into charm baryons than charm mesons. The ratio is better described by the PYTHIA 8 simulations with the CR-BLC Mode 2 compared to the ones with the Monash tune, with the former describing the data with 88% probability compared to a 0.03% probability for the latter.

In summary the first measurement in hadronic collisions of the longitudinal momentum fraction of the charged jet carried by Λ_c^+ baryons was presented for pp collisions at $\sqrt{s} = 13$ TeV. The result is fully corrected to particle level and obtained in the jet and Λ_c^+ transverse momentum intervals of $7 \leq p_T^{\text{jet ch}} < 15$ GeV/c and $3 \leq p_T^{\Lambda_c^+} < 15$ GeV/c, respectively. The measurement presented in this paper hints that charm quarks have a softer fragmentation into Λ_c^+ baryons compared to D^0 mesons, in the measured kinematic interval. One possible explanation is that charm-baryon production is favored in the presence of higher particle multiplicity originating from both the jet fragmentation and the underlying event, which could be tested with future measurements of the in-jet multiplicity of Λ_c^+-tagged jets. The fragmentation of charm quarks into Λ_c^+ baryons in hadronic collisions exhibits tension with simulations tuned on e^+e^- data that employ a leading-color formalism of hadronization, such as in the Monash tune of PYTHIA 8. This occurs despite their successful description of the fragmentation of charm quarks into D^0 mesons. However, the inclusion of mechanisms sensitive to the surrounding partonic density that feature color reconnection beyond the leading-color approximation results in a

better agreement with data. This result also partially explains the p_T shape of the prompt Λ_c^+/D^0 cross section ratio [11–15,39], which shows a peak at low p_T (≈ 3 GeV/c) and is also described within uncertainties by PYTHIA 8 with the CR-BLC Mode 2 tune. The p_T trend of this ratio is driven by the fact that the Λ_c^+ baryons produced from the fragmenting charm quark carry a significantly lower fraction of the charm-quark transverse momentum than the D^0 mesons produced in a similar way.

[1] J. C. Collins, D. E. Soper, and G. F. Sterman, Factorization of hard processes in QCD, Adv. Ser. Dir. High Energy Phys. **5**, 1 (1989).

[2] R. Seuster *et al.* (Belle Collaboration), Charm hadrons from fragmentation and B decays in e^+e^- annihilation at $\sqrt{s} = 10.6$ GeV, Phys. Rev. D **73**, 032002 (2006).

[3] M. Niiyama *et al.* (Belle Collaboration), Production cross sections of hyperons and charmed baryons from e^+e^- annihilation near $\sqrt{s} = 10.52$ GeV, Phys. Rev. D **97**, 072005 (2018).

[4] R. Barate *et al.* (ALEPH Collaboration), Study of charm production in Z decays, Eur. Phys. J. C **16**, 597 (2000).

[5] ZEUS Collaboration, Measurement of the charm fragmentation function in D* photoproduction at HERA, J. High Energy Phys. 04 (2009) 082.

[6] F. D. Aaron *et al.* (H1 Collaboration), Study of charm fragmentation into $D^{*\pm}$ mesons in deep-inelastic scattering at HERA, Eur. Phys. J. C **59**, 589 (2009).

[7] S. Acharya *et al.* (ALICE Collaboration), Measurement of the production of charm jets tagged with D^0 mesons in pp collisions at $\sqrt{s} = 5.02$ and 13 TeV, J. High Energy Phys. 06 (2023) 133.

[8] S. Acharya *et al.* (ALICE Collaboration), Measurement of the production of charm jets tagged with D^0 mesons in pp collisions at $\sqrt{s} = 7$ TeV, J. High Energy Phys. 08 (2019) 133.

[9] G. Aad *et al.* (ATLAS Collaboration), Measurement of $D^{*\pm}$ meson production in jets from pp collisions at $\sqrt{s} = 7$ TeV with the ATLAS detector, Phys. Rev. D **85**, 052005 (2012).

[10] J. Adam *et al.* (ALICE Collaboration), Enhanced production of multi-strange hadrons in high-multiplicity proton-proton collisions, Nat. Phys. **13**, 535 (2017).

[11] S. Acharya *et al.* (ALICE Collaboration), Λ_c^+ production in pp collisions at $\sqrt{s} = 7$ TeV and in p–Pb collisions at $\sqrt{s_{NN}} = 5.02$ TeV, J. High Energy Phys. 04 (2018) 108.

[12] S. Acharya *et al.* (ALICE Collaboration), Λ_c^+ production and baryon-to-meson ratios in pp and p–Pb collisions at $\sqrt{s_{NN}} = 5.02$ TeV at the LHC, Phys. Rev. Lett. **127**, 202301 (2021).

[13] S. Acharya *et al.* (ALICE Collaboration), Measurement of prompt D^0, Λ_c^+, and $\Sigma_c^{0,++}(2455)$ production in proton–proton collisions at $\sqrt{s} = 13$ TeV, Phys. Rev. Lett. **128**, 012001 (2022).

[14] S. Acharya *et al.* (ALICE Collaboration), Λ_c^+ production in pp and in p–Pb collisions at $\sqrt{s_{NN}} = 5.02$ TeV, Phys. Rev. C **104**, 054905 (2021).

[15] S. Acharya *et al.* (ALICE Collaboration), Observation of a multiplicity dependence in the p_T-differential charm baryon-to-meson ratios in proton–proton collisions at $\sqrt{s} = 13$ TeV, Phys. Lett. B **829**, 137065 (2022).

[16] S. Acharya *et al.* (ALICE Collaboration), Charm-quark fragmentation fractions and production cross section at

midrapidity in pp collisions at the LHC, Phys. Rev. D **105**, L011103 (2022).

[17] S. Acharya *et al.* (ALICE Collaboration), First measurement of Ω_c^0 production in pp collisions at $\sqrt{s} = 13$ TeV, Phys. Lett. B **846**, 137625 (2023).

[18] S. Acharya *et al.* (ALICE Collaboration), First measurement of Ξ_c^0 production in pp collisions at $\sqrt{s} = 7$ TeV, Phys. Lett. B **781**, 8 (2018).

[19] S. Acharya *et al.* (ALICE Collaboration), Measurement of the cross sections of Ξ_c^0 and Ξ_c^+ baryons and of the branching-fraction ratio $BR(\Xi_c^0 \to \Xi^- e^+ \nu_e)/BR(\Xi_c^0 \to \Xi^- \pi^+)$ in pp collisions at 13 TeV, Phys. Rev. Lett. **127**, 272001 (2021).

[20] P. Skands, S. Carrazza, and J. Rojo, Tuning PYTHIA 8.1: The Monash 2013 tune, Eur. Phys. J. C **74**, 3024 (2014).

[21] T. Sjöstrand, S. Ask, J. R. Christiansen, R. Corke, N. Desai, P. Ilten, S. Mrenna, S. Prestel, C. O. Rasmussen, and P. Z. Skands, An introduction to PYTHIA 8.2, Comput. Phys. Commun. **191**, 159 (2015).

[22] M. Bahr *et al.*, Herwig++ physics and manual, Eur. Phys. J. C **58**, 639 (2008).

[23] J. R. Christiansen and P. Z. Skands, String formation beyond leading colour, J. High Energy Phys. 08 (2015) 003.

[24] K. Aamodt *et al.* (ALICE Collaboration), The ALICE experiment at the CERN LHC, J. Instrum. **3**, S08002 (2008).

[25] ALICE Collaboration, Performance of the ALICE experiment at the CERN LHC, Int. J. Mod. Phys. A **29**, 1430044 (2014).

[26] S. Acharya *et al.* (ALICE Collaboration), ALICE 2016-2017-2018 luminosity determination for pp collisions at $\sqrt{s} = 13$ TeV, https://cds.cern.ch/record/2776672.

[27] P. Zyla *et al.* (Particle Data Group), Review of particle physics, Prog. Theor. Exp. Phys. **2020**, 083C01 (2020).

[28] T. Chen and C. Guestrin, XGBoost: A scalable tree boosting system, in *Proceedings of the 22nd ACM SIGKDD International Conference on Knowledge Discovery and Data Mining*, KDD '16 (Association for Computing Machinery, New York, NY, 2016), pp. 785–794, arXiv:1603.02754.

[29] R. Brun, F. Bruyant, M. Maire, A. C. McPherson, and P. Zanarini, Geant 3: User's guide Geant 3.10, Geant 3.11; rev. version (CERN, Geneva, 1987), https://cds.cern.ch/record/1119728.

[30] M. Cacciari, G. P. Salam, and G. Soyez, FastJet user manual, Eur. Phys. J. C **72**, 1896 (2012).

[31] M. Cacciari, G. P. Salam, and G. Soyez, The anti-k_t jet clustering algorithm, J. High Energy Phys. 04 (2008) 063.

[32] M. Cacciari, G. P. Salam, and G. Soyez, The catchment area of jets, J. High Energy Phys. 04 (2008) 005.

[33] K. C. Han, R. J. Fries, and C. M. Ko, Jet fragmentation via recombination of parton showers, Phys. Rev. C **93**, 045207 (2016).

[34] S. Alioli, P. Nason, C. Oleari, and E. Re, A general framework for implementing NLO calculations in shower Monte Carlo programs: The POWHEG BOX, J. High Energy Phys. 06 (2010) 043.

[35] T. Sjöstrand, S. Mrenna, and P. Z. Skands, PYTHIA 6.4 physics and manual, J. High Energy Phys. 05 (2006) 026.

[36] D. J. Lange, The EvtGen particle decay simulation package, Nucl. Instrum. Methods Phys. Res., Sect. A **462**, 152 (2001).

[37] G. D'Agostini, A multidimensional unfolding method based on Bayes' theorem, Nucl. Instrum. Methods Phys. Res., Sect. A **362**, 487 (1995).

[38] M. Cacciari, P. Nason, and R. Vogt, QCD predictions for charm and bottom quark production at RHIC, Phys. Rev. Lett. **95**, 122001 (2005).

[39] A. M. Sirunyan *et al.* (CMS Collaboration), Production of Λ_c^+ baryons in proton-proton and lead-lead collisions at $\sqrt{s_{NN}} = 5.02$ TeV, Phys. Lett. B **803**, 135328 (2020).

S. Acharya[126] D. Adamová[86] A. Adler,[70] G. Aglieri Rinella[32] M. Agnello[29] N. Agrawal[51] Z. Ahammed[134] S. Ahmad[15] S. U. Ahn[71] I. Ahuja[37] A. Akindinov[140] M. Al-Turany[97] D. Aleksandrov[140] B. Alessandro[56] H. M. Alfanda[6] R. Alfaro Molina[67] B. Ali[15] A. Alici[25a,25b] N. Alizadehvandchali[115] A. Alkin[32] J. Alme[20] G. Alocco[52] T. Alt[64] I. Altsybeev[140] J. R. Alvarado[44] M. N. Anaam[6] C. Andrei[45] A. Andronic[125] V. Anguelov[94] F. Antinori[54] P. Antonioli[51] N. Apadula[74] L. Aphecetche[103] H. Appelshäuser[64] C. Arata[73] S. Arcelli[25a,25b] M. Aresti[52] R. Arnaldi[56] J. G. M. C. A. Arneiro[110] I. C. Arsene[19] M. Arslandok[137] A. Augustinus[32] R. Averbeck[97] M. D. Azmi[15] A. Badalà[53] J. Bae[104] Y. W. Baek[40] X. Bai[119] R. Bailhache[64] Y. Bailung[48] A. Balbino[29] A. Baldisseri[129] B. Balis[2] D. Banerjee[4a,4b] Z. Banoo[91] R. Barbera[26a,26b] F. Barile[31a,31b] L. Barioglio[95] M. Barlou,[78] G. G. Barnaföldi[46] L. S. Barnby[85] V. Barret[126] L. Barreto[110] C. Bartels[118] K. Barth[32] E. Bartsch[64] N. Bastid[126] S. Basu[75] G. Batigne[103] D. Battistini[95] B. Batyunya[141] D. Bauri,[47] J. L. Bazo Alba[101] I. G. Bearden[83] C. Beattie[137] P. Becht[97] D. Behera[48] I. Belikov[128] A. D. C. Bell Hechavarria[125] F. Bellini[25a,25b] R. Bellwied[115] S. Belokurova[140] V. Belyaev[140] G. Bencedi[46] S. Beole[24a,24b] A. Bercuci[45] Y. Berdnikov[140] A. Berdnikova[94] L. Bergmann[94] M. G. Besoiu[63] L. Betev[32] P. P. Bhaduri[134] A. Bhasin[91] M. A. Bhat[4a,4b] B. Bhattacharjee[41] L. Bianchi[24a,24b] N. Bianchi[49] J. Bielčík[35] J. Bielčíková[86] J. Biernat[107] A. P. Bigot[128] A. Bilandzic[95] G. Biro[46] S. Biswas[4a,4b] N. Bize[103] J. T. Blair[108] D. Blau[140] M. B. Blidaru[97] N. Bluhme,[38] C. Blume[64] G. Boca[21,55] F. Bock[87] T. Bodova[20]

A. Bogdanov,[140] S. Boi,[22a,22b] J. Bok,[58] L. Boldizsár,[46] M. Bombara,[37] P. M. Bond,[32] G. Bonomi,[55,133] H. Borel,[129] A. Borissov,[140] A. G. Borquez Carcamo,[94] H. Bossi,[137] E. Botta,[24a,24b] Y. E. M. Bouziani,[64] L. Bratrud,[64] P. Braun-Munzinger,[97] M. Bregant,[110] M. Broz,[35] G. E. Bruno,[31a,31b,96] M. D. Buckland,[23a,23b] D. Budnikov,[140] H. Buesching,[64] S. Bufalino,[29] O. Bugnon,[103] P. Buhler,[102] Z. Buthelezi,[68,122] S. A. Bysiak,[107] M. Cai,[6] H. Caines,[137] A. Caliva,[97] E. Calvo Villar,[101] J. M. M. Camacho,[109] P. Camerini,[23a,23b] F. D. M. Canedo,[110] S. L. Cantway,[137] M. Carabas,[113] A. A. Carballo,[32] F. Carnesecchi,[32] R. Caron,[127] L. A. D. Carvalho,[110] J. Castillo Castellanos,[129] F. Catalano,[24a,24b] C. Ceballos Sanchez,[141] I. Chakaberia,[74] P. Chakraborty,[47] S. Chandra,[134] S. Chapeland,[32] M. Chartier,[118] S. Chattopadhyay,[134] S. Chattopadhyay,[99] T. Cheng,[6,97] C. Cheshkov,[127] B. Cheynis,[127] V. Chibante Barroso,[32] D. D. Chinellato,[111] E. S. Chizzali,[95,‡] J. Cho,[58] S. Cho,[58] P. Chochula,[32] P. Christakoglou,[84] C. H. Christensen,[83] P. Christiansen,[75] T. Chujo,[124] M. Ciacco,[29] C. Cicalo,[52] F. Cindolo,[51] M. R. Ciupek,[97] G. Clai,[51,§] F. Colamaria,[50] J. S. Colburn,[100] D. Colella,[31a,31b,96] M. Colocci,[32] M. Concas,[56,∥] G. Conesa Balbastre,[73] Z. Conesa del Valle,[130] G. Contin,[23a,23b] J. G. Contreras,[35] M. L. Coquet,[129] T. M. Cormier,[87,†] P. Cortese,[56,132] M. R. Cosentino,[112] F. Costa,[32] S. Costanza,[21,55] C. Cot,[130] J. Crkovská,[94] P. Crochet,[126] R. Cruz-Torres,[74] E. Cuautle,[65] P. Cui,[6] A. Dainese,[54] M. C. Danisch,[94] A. Danu,[63] P. Das,[80] P. Das,[4a,4b] S. Das,[4a,4b] A. R. Dash,[125] S. Dash,[47] A. De Caro,[28a,28b] G. de Cataldo,[50] J. de Cuveland,[38] A. De Falco,[22a,22b] D. De Gruttola,[28a,28b] N. De Marco,[56] C. De Martin,[23a,23b] S. De Pasquale,[28a,28b] S. Deb,[48] R. J. Debski,[2] K. R. Deja,[135] R. Del Grande,[95] L. Dello Stritto,[28a,28b] W. Deng,[6] P. Dhankher,[18] D. Di Bari,[31a,31b] A. Di Mauro,[32] R. A. Diaz,[7,141] T. Dietel,[114] Y. Ding,[6,127] R. Divià,[32] D. U. Dixit,[18] Ø. Djuvsland,[20] U. Dmitrieva,[140] A. Dobrin,[63] B. Dönigus,[64] J. M. Dubinski,[135] A. Dubla,[97] S. Dudi,[90] P. Dupieux,[126] M. Durkac,[106] N. Dzalaiova,[12] T. M. Eder,[125] R. J. Ehlers,[87] V. N. Eikeland,[20] F. Eisenhut,[64] D. Elia,[50] B. Erazmus,[103] F. Ercolessi,[25a,25b] F. Erhardt,[89] M. R. Ersdal,[20] B. Espagnon,[130] G. Eulisse,[32] D. Evans,[100] S. Evdokimov,[140] L. Fabbietti,[95] M. Faggin,[27a,27b] J. Faivre,[73] F. Fan,[6] W. Fan,[74] A. Fantoni,[49] M. Fasel,[87] P. Fecchio,[29] A. Feliciello,[56] G. Feofilov,[140] A. Fernández Téllez,[44] L. Ferrandi,[110] M. B. Ferrer,[32] A. Ferrero,[129] C. Ferrero,[56] A. Ferretti,[24a,24b] V. J. G. Feuillard,[94] V. Filova,[35] D. Finogeev,[140] F. M. Fionda,[52] F. Flor,[115] A. N. Flores,[108] S. Foertsch,[68] I. Fokin,[94] S. Fokin,[140] E. Fragiacomo,[57] E. Frajna,[46] U. Fuchs,[32] N. Funicello,[28a,28b] C. Furget,[73] A. Furs,[140] T. Fusayasu,[98] J. J. Gaardhøje,[83] M. Gagliardi,[24a,24b] A. M. Gago,[101] C. D. Galvan,[109] D. R. Gangadharan,[115] P. Ganoti,[78] C. Garabatos,[97] T. García Chávez,[44] E. Garcia-Solis,[9] K. Garg,[103] C. Gargiulo,[32] K. Garner,[125] P. Gasik,[97] A. Gautam,[117] M. B. Gay Ducati,[66] M. Germain,[103] A. Ghimouz,[124] C. Ghosh,[134] M. Giacalone,[25a,25b,51] P. Giubellino,[56,97] P. Giubilato,[27a,27b] A. M. C. Glaenzer,[129] P. Glässel,[94] E. Glimos,[121] D. J. Q. Goh,[76] V. Gonzalez,[136] L. H. González-Trueba,[67] M. Gorgon,[2] S. Gotovac,[33] V. Grabski,[67] L. K. Graczykowski,[135] E. Grecka,[86] A. Grelli,[59] C. Grigoras,[32] V. Grigoriev,[140] S. Grigoryan,[1,141] F. Grosa,[32] J. F. Grosse-Oetringhaus,[32] R. Grosso,[97] D. Grund,[35] G. G. Guardiano,[111] R. Guernane,[73] M. Guilbaud,[103] K. Gulbrandsen,[83] T. Gündem,[64] T. Gunji,[123] W. Guo,[6] A. Gupta,[91] R. Gupta,[91] L. Gyulai,[46] M. K. Habib,[97] C. Hadjidakis,[130] F. U. Haider,[91] H. Hamagaki,[76] A. Hamdi,[74] M. Hamid,[6] Y. Han,[138] R. Hannigan,[108] M. R. Haque,[135] J. W. Harris,[137] A. Harton,[9] H. Hassan,[87] D. Hatzifotiadou,[51] P. Hauer,[42] L. B. Havener,[137] S. T. Heckel,[95] E. Hellbär,[97] H. Helstrup,[34] M. Hemmer,[64] T. Herman,[35] G. Herrera Corral,[8] F. Herrmann,[125] S. Herrmann,[127] K. F. Hetland,[34] B. Heybeck,[64] H. Hillemanns,[32] C. Hills,[118] B. Hippolyte,[128] F. W. Hoffmann,[70] B. Hofman,[59] B. Hohlweger,[84] G. H. Hong,[138] M. Horst,[95] A. Horzyk,[2] Y. Hou,[6] P. Hristov,[32] C. Hughes,[121] P. Huhn,[64] L. M. Huhta,[116] T. J. Humanic,[88] A. Hutson,[115] D. Hutter,[38] J. P. Iddon,[118] R. Ilkaev,[140] H. Ilyas,[13] M. Inaba,[124] G. M. Innocenti,[32] M. Ippolitov,[140] A. Isakov,[86] T. Isidori,[117] M. S. Islam,[99] M. Ivanov,[97] M. Ivanov,[12] V. Ivanov,[140] M. Jablonski,[2] B. Jacak,[74] N. Jacazio,[32] P. M. Jacobs,[74] S. Jadlovska,[106] J. Jadlovsky,[106] S. Jaelani,[82] L. Jaffe,[38] C. Jahnke,[111] M. J. Jakubowska,[135] M. A. Janik,[135] T. Janson,[70] M. Jercic,[89] S. Jia,[10] A. A. P. Jimenez,[65] F. Jonas,[87,125] J. M. Jowett,[32,97] J. Jung,[64] M. Jung,[64] A. Junique,[32] A. Jusko,[100] M. J. Kabus,[32,135] J. Kaewjai,[105] P. Kalinak,[60] A. S. Kalteyer,[97] A. Kalweit,[32] V. Kaplin,[140] A. Karasu Uysal,[72] D. Karatovic,[89] O. Karavichev,[140] T. Karavicheva,[140] P. Karczmarczyk,[135] E. Karpechev,[140] U. Kebschull,[70] R. Keidel,[139] D. L. D. Keijdener,[59] M. Keil,[32] B. Ketzer,[42] A. M. Khan,[6] S. Khan,[15] A. Khanzadeev,[140] Y. Kharlov,[140] A. Khatun,[15,117] A. Khuntia,[107] M. B. Kidson,[114] B. Kileng,[34] B. Kim,[16] C. Kim,[16] D. J. Kim,[116] E. J. Kim,[69] J. Kim,[138] J. S. Kim,[40] J. Kim,[69] M. Kim,[18,94] S. Kim,[17] T. Kim,[138] K. Kimura,[92] S. Kirsch,[64] I. Kisel,[38] S. Kiselev,[140]

A. Kisiel[135] J. P. Kitowski[2] J. L. Klay[5] J. Klein[32] S. Klein[74] C. Klein-Bösing[125] M. Kleiner[64] T. Klemenz[95] A. Kluge[32] A. G. Knospe[115] C. Kobdaj[105] T. Kollegger[97] A. Kondratyev[141] N. Kondratyeva[140] E. Kondratyuk[140] J. Konig[64] S. A. Konigstorfer[95] P. J. Konopka[32] G. Kornakov[135] M. Korwieser[95] S. D. Koryciak[2] A. Kotliarov[86] V. Kovalenko[140] M. Kowalski[107] V. Kozhuharov[36] I. Králik[60] A. Kravčáková[37] L. Kreis[97] M. Krivda[60,100] F. Krizek[86] K. Krizkova Gajdosova[35] M. Kroesen[94] M. Krüger[64] D. M. Krupova[35] E. Kryshen[140] V. Kučera[32] C. Kuhn[128] P. G. Kuijer[84] T. Kumaoka[124] D. Kumar[134] L. Kumar[90] N. Kumar[90] S. Kumar[31a,31b] S. Kundu[32] P. Kurashvili[79] A. Kurepin[140] A. B. Kurepin[140] A. Kuryakin[140] S. Kushpil[86] J. Kvapil[100] M. J. Kweon[58] J. Y. Kwon[58] Y. Kwon[138] S. L. La Pointe[38] P. La Rocca[26a,26b] Y. S. Lai[74] A. Lakrathok[105] M. Lamanna[32] R. Langoy[120] P. Larionov[32] E. Laudi[32] L. Lautner[32,95] R. Lavicka[102] T. Lazareva[140] R. Lea[55,133] H. Lee[104] G. Legras[125] J. Lehrbach[38] R. C. Lemmon[85] I. León Monzón[109] M. M. Lesch[95] E. D. Lesser[18] M. Lettrich[95] P. Lévai[46] X. Li[10] X. L. Li[6] J. Lien[120] R. Lietava[100] I. Likmeta[115] B. Lim[16,24a,24b] S. H. Lim[16] V. Lindenstruth[38] A. Lindner[45] C. Lippmann[97] A. Liu[18] D. H. Liu[6] J. Liu[118] I. M. Lofnes[20] C. Loizides[87] S. Lokos[107] J. Lömker[59] P. Loncar[33] J. A. Lopez[94] X. Lopez[126] E. López Torres[7] P. Lu[97,119] J. R. Luhder[125] M. Lunardon[27a,27b] G. Luparello[57] Y. G. Ma[39] A. Maevskaya[140] M. Mager[32] T. Mahmoud[42] A. Maire[128] M. V. Makariev[36] M. Malaev[140] G. Malfattore[25a,25b] N. M. Malik[91] Q. W. Malik[19] S. K. Malik[91] L. Malinina[141,†,¶] D. Mal'Kevich[140] D. Mallick[80] N. Mallick[48] G. Mandaglio[30,53] V. Manko[140] F. Manso[126] V. Manzari[50] Y. Mao[6] G. V. Margagliotti[23a,23b] A. Margotti[51] A. Marín[97] C. Markert[108] P. Martinengo[32] J. L. Martinez[115] M. I. Martínez[44] G. Martínez García[103] S. Masciocchi[97] M. Masera[24a,24b] A. Masoni[52] L. Massacrier[130] A. Mastroserio[50,131] O. Matonoha[75] P. F. T. Matuoka[110] A. Matyja[107] C. Mayer[107] A. L. Mazuecos[32] F. Mazzaschi[24a,24b] M. Mazzilli[32] J. E. Mdhluli[122] A. F. Mechler[64] Y. Melikyan[43,140] A. Menchaca-Rocha[67] E. Meninno[102] A. S. Menon[115] M. Meres[12] S. Mhlanga[68,114] Y. Miake[124] L. Micheletti[56] L. C. Migliorin[127] D. L. Mihaylov[95] K. Mikhaylov[140,141] A. N. Mishra[46] D. Miśkowiec[97] A. Modak[4a,4b] A. P. Mohanty[59] B. Mohanty[80] M. Mohisin Khan[15,**] M. A. Molander[43] Z. Moravcova[83] C. Mordasini[95] D. A. Moreira De Godoy[125] I. Morozov[140] A. Morsch[32] T. Mrnjavac[32] V. Muccifora[49] S. Muhuri[134] J. D. Mulligan[74] A. Mulliri[22a,22b] M. G. Munhoz[110] R. H. Munzer[64] H. Murakami[123] S. Murray[114] L. Musa[32] J. Musinsky[60] J. W. Myrcha[135] B. Naik[122] A. I. Nambrath[18] B. K. Nandi[47] R. Nania[51] E. Nappi[50] A. F. Nassirpour[75] A. Nath[94] C. Nattrass[121] M. N. Naydenov[36] A. Neagu[19] A. Negru[113] L. Nellen[65] S. V. Nesbo[34] G. Neskovic[38] D. Nesterov[140] B. S. Nielsen[83] E. G. Nielsen[83] S. Nikolaev[140] S. Nikulin[140] V. Nikulin[140] F. Noferini[51] S. Noh[11] P. Nomokonov[141] J. Norman[118] N. Novitzky[124] P. Nowakowski[135] A. Nyanin[140] J. Nystrand[20] M. Ogino[76] A. Ohlson[75] V. A. Okorokov[140] J. Oleniacz[135] A. C. Oliveira Da Silva[121] M. H. Oliver[137] A. Onnerstad[116] C. Oppedisano[56] A. Ortiz Velasquez[65] J. Otwinowski[107] M. Oya[92] K. Oyama[76] Y. Pachmayer[94] S. Padhan[47] D. Pagano[55,133] G. Paić[65] S. Paisano-Guzmán[44] A. Palasciano[50] S. Panebianco[129] H. Park[124] H. Park[104] J. Park[58] J. E. Parkkila[32] R. N. Patra[91] B. Paul[22a,22b] H. Pei[6] T. Peitzmann[59] X. Peng[6] M. Pennisi[24a,24b] L. G. Pereira[66] D. Peresunko[140] G. M. Perez[7] S. Perrin[129] Y. Pestov[140] V. Petráček[35] V. Petrov[140] M. Petrovici[45] R. P. Pezzi[66,103] S. Piano[57] M. Pikna[12] P. Pillot[103] O. Pinazza[32,51] L. Pinsky[115] C. Pinto[95] S. Pisano[49] M. Płoskoń[74] M. Planinic[89] F. Pliquett[64] M. G. Poghosyan[87] B. Polichtchouk[140] S. Politano[29] N. Poljak[89] A. Pop[45] S. Porteboeuf-Houssais[126] V. Pozdniakov[141] K. K. Pradhan[48] S. K. Prasad[4a,4b] S. Prasad[48] R. Preghenella[51] F. Prino[56] C. A. Pruneau[136] I. Pshenichnov[140] M. Puccio[32] S. Pucillo[24a,24b] Z. Pugelova[106] S. Qiu[84] L. Quaglia[24a,24b] R. E. Quishpe[115] S. Ragoni[14,100] A. Rakotozafindrabe[129] L. Ramello[56,132] F. Rami[128] T. A. Rancien[73] M. Rasa[26a,26b] S. S. Räsänen[43] R. Rath[51] M. P. Rauch[20] I. Ravasenga[84] K. F. Read[87,121] C. Reckziegel[112] A. R. Redelbach[38] K. Redlich[79,†] C. A. Reetz[97] H. D. Regules-Medel[44] A. Rehman[20] F. Reidt[32] H. A. Reme-Ness[34] Z. Rescakova[37] K. Reygers[94] A. Riabov[140] V. Riabov[140] R. Ricci[28a,28b] M. Richter[19] A. A. Riedel[95] W. Riegler[32] C. Ristea[63] M. Rodríguez Cahuantzi[44] S. A. Rodríguez Ramírez[44] K. Røed[19] R. Rogalev[140] E. Rogochaya[141] T. S. Rogoschinski[64] D. Rohr[32] D. Röhrich[20] P. F. Rojas[44] S. Rojas Torres[35] P. S. Rokita[135] G. Romanenko[141] F. Ronchetti[49] A. Rosano[30,53] E. D. Rosas[65] K. Roslon[135] A. Rossi[54] A. Roy[48] S. Roy[47] N. Rubini[25a,25b] D. Ruggiano[135] R. Rui[23a,23b] B. Rumyantsev[141] P. G. Russek[2] R. Russo[84] A. Rustamov[81] E. Ryabinkin[140] Y. Ryabov[140] A. Rybicki[107]

H. Rytkonen[116] W. Rzesa[135] O. A. M. Saarimaki[43] R. Sadek[103] S. Sadhu[31a,31b] S. Sadovsky[140] J. Saetre[20] K. Šafařík[35] S. K. Saha[4a,4b] S. Saha[80] B. Sahoo[47] R. Sahoo[48] S. Sahoo[61] D. Sahu[48] P. K. Sahu[61] J. Saini[134] K. Sajdakova[37] S. Sakai[124] M. P. Salvan[97] S. Sambyal[91] I. Sanna[32,95] T. B. Saramela[110] D. Sarkar[136] N. Sarkar[134] P. Sarma[41] V. Sarritzu[22a,22b] V. M. Sarti[95] M. H. P. Sas[137] J. Schambach[87] H. S. Scheid[64] C. Schiaua[45] R. Schicker[94] A. Schmah[94] C. Schmidt[97] H. R. Schmidt[93] M. O. Schmidt[32] M. Schmidt[93] N. V. Schmidt[87] A. R. Schmier[121] R. Schotter[128] A. Schröter[38] J. Schukraft[32] K. Schwarz[97] K. Schweda[97] G. Scioli[25a,25b] E. Scomparin[56] J. E. Seger[14] Y. Sekiguchi[123] D. Sekihata[123] I. Selyuzhenkov[97,140] S. Senyukov[128] J. J. Seo[58] D. Serebryakov[140] L. Šerkšnytė[95] A. Sevcenco[63] T. J. Shaba[68] A. Shabetai[103] R. Shahoyan[32] A. Shangaraev[140] A. Sharma[90] B. Sharma[91] D. Sharma[47] H. Sharma[107] M. Sharma[91] S. Sharma[76] S. Sharma[91] U. Sharma[91] A. Shatat[130] O. Sheibani[115] K. Shigaki[92] M. Shimomura[77] J. Shin[11] S. Shirinkin[140] Q. Shou[39] Y. Sibiriak[140] S. Siddhanta[52] T. Siemiarczuk[79] T. F. Silva[110] D. Silvermyr[75] T. Simantathammakul[105] R. Simeonov[36] B. Singh[91] B. Singh[95] R. Singh[80] R. Singh[91] R. Singh[48] S. Singh[15] V. K. Singh[134] V. Singhal[134] T. Sinha[99] B. Sitar[12] M. Sitta[56,132] T. B. Skaali[19] G. Skorodumovs[94] M. Slupecki[43] N. Smirnov[137] R. J. M. Snellings[59] E. H. Solheim[19] J. Song[115] A. Songmoolnak[105] F. Soramel[27a,27b] R. Spijkers[84] I. Sputowska[107] J. Staa[75] J. Stachel[94] I. Stan[63] P. J. Steffanic[121] S. F. Stiefelmaier[94] D. Stocco[103] I. Storehaug[19] P. Stratmann[125] S. Strazzi[25a,25b] C. P. Stylianidis[84] A. A. P. Suaide[110] C. Suire[130] M. Sukhanov[140] M. Suljic[32] R. Sultanov[140] V. Sumberia[91] S. Sumowidagdo[82] S. Swain[61] I. Szarka[12] M. Szymkowski[135] S. F. Taghavi[95] G. Taillepied[97] J. Takahashi[111] G. J. Tambave[20] S. Tang[6,126] Z. Tang[119] J. D. Tapia Takaki[117] N. Tapus[113] L. A. Tarasovicova[125] M. G. Tarzila[45] G. F. Tassielli[31a,31b] A. Tauro[32] G. Tejeda Muñoz[44] A. Telesca[32] L. Terlizzi[24a,24b] C. Terrevoli[115] G. Tersimonov[3] S. Thakur[4a,4b] D. Thomas[108] A. Tikhonov[140] A. R. Timmins[115] M. Tkacik[106] T. Tkacik[106] A. Toia[64] R. Tokumoto[92] N. Topilskaya[140] M. Toppi[49] F. Torales-Acosta[18] T. Tork[130] A. G. Torres Ramos[31a,31b] A. Trifiró[30,53] A. S. Triolo[30,53] S. Tripathy[51] T. Tripathy[47] S. Trogolo[32] V. Trubnikov[3] W. H. Trzaska[116] T. P. Trzcinski[135] A. Tumkin[140] R. Turrisi[54] T. S. Tveter[19] K. Ullaland[20] B. Ulukutlu[95] A. Uras[127] M. Urioni[55,133] G. L. Usai[22a,22b] M. Vala[37] N. Valle[21] L. V. R. van Doremalen[59] C. Van Hulse[130] M. van Leeuwen[84] C. A. van Veen[94] R. J. G. van Weelden[84] P. Vande Vyvre[32] D. Varga[46] Z. Varga[46] M. Vasileiou[78] A. Vasiliev[140] O. Vázquez Doce[49] O. Vazquez Rueda[75,115] V. Vechernin[140] E. Vercellin[24a,24b] S. Vergara Limón[44] L. Vermunt[97] R. Vértesi[46] M. Verweij[59] L. Vickovic[33] Z. Vilakazi[122] O. Villalobos Baillie[100] A. Villani[23a,23b] G. Vino[50] A. Vinogradov[140] T. Virgili[28a,28b] V. Vislavicius[75] A. Vodopyanov[141] B. Volkel[32] M. A. Völkl[94] K. Voloshin[140] S. A. Voloshin[136] G. Volpe[31a,31b] B. von Haller[32] I. Vorobyev[95] N. Vozniuk[140] J. Vrláková[37] C. Wang[39] D. Wang[39] Y. Wang[39] A. Wegrzynek[32] F. T. Weiglhofer[38] S. C. Wenzel[32] J. P. Wessels[125] J. Wiechula[64] J. Wikne[19] G. Wilk[79] J. Wilkinson[97] G. A. Willems[125] B. Windelband[94] M. Winn[129] J. R. Wright[108] W. Wu[39] Y. Wu[119] R. Xu[6] A. Yadav[42] A. K. Yadav[134] S. Yalcin[72] Y. Yamaguchi[92] S. Yang[20] S. Yano[92] Z. Yin[6] I.-K. Yoo[16] J. H. Yoon[58] S. Yuan[20] A. Yuncu[94] V. Zaccolo[23a,23b] C. Zampolli[32] F. Zanone[94] N. Zardoshti[32,100] A. Zarochentsev[140] P. Závada[62] N. Zaviyalov[140] M. Zhalov[140] B. Zhang[6] L. Zhang[39] S. Zhang[39] X. Zhang[6] Y. Zhang[119] Z. Zhang[6] M. Zhao[10] V. Zherebchevskii[140] Y. Zhi[10] D. Zhou[6] Y. Zhou[83] J. Zhu[6,97] Y. Zhu[6] S. C. Zugravel[56] and N. Zurlo[55,133]

(ALICE Collaboration)

[1]*A.I. Alikhanyan National Science Laboratory (Yerevan Physics Institute) Foundation, Yerevan, Armenia*
[2]*AGH University of Krakow, Cracow, Poland*
[3]*Bogolyubov Institute for Theoretical Physics, National Academy of Sciences of Ukraine, Kiev, Ukraine*
[4a]*Bose Institute, Department of Physics, Kolkata, India*
[4b]*Centre for Astroparticle Physics and Space Science (CAPSS), Kolkata, India*
[5]*California Polytechnic State University, San Luis Obispo, California, USA*
[6]*Central China Normal University, Wuhan, China*
[7]*Centro de Aplicaciones Tecnológicas y Desarrollo Nuclear (CEADEN), Havana, Cuba*
[8]*Centro de Investigación y de Estudios Avanzados (CINVESTAV), Mexico City and Mérida, Mexico*
[9]*Chicago State University, Chicago, Illinois, USA*

[10]China Institute of Atomic Energy, Beijing, China

[11]Chungbuk National University, Cheongju, Republic of Korea

[12]Comenius University Bratislava, Faculty of Mathematics, Physics and Informatics, Bratislava, Slovak Republic

[13]COMSATS University Islamabad, Islamabad, Pakistan

[14]Creighton University, Omaha, Nebraska, USA

[15]Department of Physics, Aligarh Muslim University, Aligarh, India

[16]Department of Physics, Pusan National University, Pusan, Republic of Korea

[17]Department of Physics, Sejong University, Seoul, Republic of Korea

[18]Department of Physics, University of California, Berkeley, California, USA

[19]Department of Physics, University of Oslo, Oslo, Norway

[20]Department of Physics and Technology, University of Bergen, Bergen, Norway

[21]Dipartimento di Fisica, Università di Pavia, Pavia, Italy

[22a]Dipartimento di Fisica dell'Università, Cagliari, Italy

[22b]Sezione INFN, Cagliari, Italy

[23a]Dipartimento di Fisica dell'Università, Trieste, Italy

[23b]Sezione INFN, Trieste, Italy

[24a]Dipartimento di Fisica dell'Università, Turin, Italy

[24b]Sezione INFN, Turin, Italy

[25a]Dipartimento di Fisica e Astronomia dell'Università, Bologna, Italy

[25b]Sezione INFN, Bologna, Italy

[26a]Dipartimento di Fisica e Astronomia dell'Università, Catania, Italy

[26b]Sezione INFN, Catania, Italy

[27a]Dipartimento di Fisica e Astronomia dell'Università, Padova, Italy

[27b]Sezione INFN, Padova, Italy

[28a]Dipartimento di Fisica "E.R. Caianiello" dell'Università, Salerno, Italy

[28b]Gruppo Collegato INFN, Salerno, Italy

[29]Dipartimento DISAT del Politecnico and Sezione INFN, Turin, Italy

[30]Dipartimento di Scienze MIFT, Università di Messina, Messina, Italy

[31a]Dipartimento Interateneo di Fisica "M. Merlin," Bari, Italy

[31b]Sezione INFN, Bari, Italy

[32]European Organization for Nuclear Research (CERN), Geneva, Switzerland

[33]Faculty of Electrical Engineering, Mechanical Engineering and Naval Architecture, University of Split, Split, Croatia

[34]Faculty of Engineering and Science, Western Norway University of Applied Sciences, Bergen, Norway

[35]Faculty of Nuclear Sciences and Physical Engineering, Czech Technical University in Prague, Prague, Czech Republic

[36]Faculty of Physics, Sofia University, Sofia, Bulgaria

[37]Faculty of Science, P.J. Šafárik University, Košice, Slovak Republic

[38]Frankfurt Institute for Advanced Studies, Johann Wolfgang Goethe-Universität Frankfurt, Frankfurt, Germany

[39]Fudan University, Shanghai, China

[40]Gangneung-Wonju National University, Gangneung, Republic of Korea

[41]Gauhati University, Department of Physics, Guwahati, India

[42]Helmholtz-Institut für Strahlen- und Kernphysik, Rheinische Friedrich-Wilhelms-Universität Bonn, Bonn, Germany

[43]Helsinki Institute of Physics (HIP), Helsinki, Finland

[44]High Energy Physics Group, Universidad Autónoma de Puebla, Puebla, Mexico

[45]Horia Hulubei National Institute of Physics and Nuclear Engineering, Bucharest, Romania

[46]HUN-REN Wigner Research Centre for Physics, Budapest, Hungary

[47]Indian Institute of Technology Bombay (IIT), Mumbai, India

[48]Indian Institute of Technology Indore, Indore, India

[49]INFN, Laboratori Nazionali di Frascati, Frascati, Italy

[50]INFN, Sezione di Bari, Bari, Italy

[51]INFN, Sezione di Bologna, Bologna, Italy

[52]INFN, Sezione di Cagliari, Cagliari, Italy

[53]INFN, Sezione di Catania, Catania, Italy

[54]INFN, Sezione di Padova, Padova, Italy

[55]INFN, Sezione di Pavia, Pavia, Italy

[56]INFN, Sezione di Torino, Turin, Italy

[57]INFN, Sezione di Trieste, Trieste, Italy

[58]Inha University, Incheon, Republic of Korea

[59]Institute for Gravitational and Subatomic Physics (GRASP), Utrecht University/Nikhef, Utrecht, Netherlands

[60]Institute of Experimental Physics, Slovak Academy of Sciences, Košice, Slovak Republic

[61]Institute of Physics, Homi Bhabha National Institute, Bhubaneswar, India

[62]Institute of Physics of the Czech Academy of Sciences, Prague, Czech Republic

[63]Institute of Space Science (ISS), Bucharest, Romania

[64]Institut für Kernphysik, Johann Wolfgang Goethe-Universität Frankfurt, Frankfurt, Germany

[65]Instituto de Ciencias Nucleares, Universidad Nacional Autónoma de México, Mexico City, Mexico

[66]Instituto de Física, Universidade Federal do Rio Grande do Sul (UFRGS), Porto Alegre, Brazil

[67]Instituto de Física, Universidad Nacional Autónoma de México, Mexico City, Mexico

[68]iThemba LABS, National Research Foundation, Somerset West, South Africa

[69]Jeonbuk National University, Jeonju, Republic of Korea

[70]Johann-Wolfgang-Goethe Universität Frankfurt Institut für Informatik, Fachbereich Informatik und Mathematik, Frankfurt, Germany

[71]Korea Institute of Science and Technology Information, Daejeon, Republic of Korea

[72]KTO Karatay University, Konya, Turkey

[73]Laboratoire de Physique Subatomique et de Cosmologie, Université Grenoble-Alpes, CNRS-IN2P3, Grenoble, France

[74]Lawrence Berkeley National Laboratory, Berkeley, California, USA

[75]Lund University Department of Physics, Division of Particle Physics, Lund, Sweden

[76]Nagasaki Institute of Applied Science, Nagasaki, Japan

[77]Nara Women's University (NWU), Nara, Japan

[78]National and Kapodistrian University of Athens, School of Science, Department of Physics, Athens, Greece

[79]National Centre for Nuclear Research, Warsaw, Poland

[80]National Institute of Science Education and Research, Homi Bhabha National Institute, Jatni, India

[81]National Nuclear Research Center, Baku, Azerbaijan

[82]National Research and Innovation Agency—BRIN, Jakarta, Indonesia

[83]Niels Bohr Institute, University of Copenhagen, Copenhagen, Denmark

[84]Nikhef, National institute for subatomic physics, Amsterdam, Netherlands

[85]Nuclear Physics Group, STFC Daresbury Laboratory, Daresbury, United Kingdom

[86]Nuclear Physics Institute of the Czech Academy of Sciences, Husinec-Řež, Czech Republic

[87]Oak Ridge National Laboratory, Oak Ridge, Tennessee, USA

[88]Ohio State University, Columbus, Ohio, USA

[89]Physics department, Faculty of science, University of Zagreb, Zagreb, Croatia

[90]Physics Department, Panjab University, Chandigarh, India

[91]Physics Department, University of Jammu, Jammu, India

[92]Physics Program and International Institute for Sustainability with Knotted Chiral Meta Matter (SKCM2), Hiroshima University, Hiroshima, Japan

[93]Physikalisches Institut, Eberhard-Karls-Universität Tübingen, Tübingen, Germany

[94]Physikalisches Institut, Ruprecht-Karls-Universität Heidelberg, Heidelberg, Germany

[95]Physik Department, Technische Universität München, Munich, Germany

[96]Politecnico di Bari and Sezione INFN, Bari, Italy

[97]Research Division and ExtreMe Matter Institute EMMI, GSI Helmholtzzentrum für Schwerionenforschung GmbH, Darmstadt, Germany

[98]Saga University, Saga, Japan

[99]Saha Institute of Nuclear Physics, Homi Bhabha National Institute, Kolkata, India

[100]School of Physics and Astronomy, University of Birmingham, Birmingham, United Kingdom

[101]Sección Física, Departamento de Ciencias, Pontificia Universidad Católica del Perú, Lima, Peru

[102]Stefan Meyer Institut für Subatomare Physik (SMI), Vienna, Austria

[103]SUBATECH, IMT Atlantique, Nantes Université, CNRS-IN2P3, Nantes, France

[104]Sungkyunkwan University, Suwon City, Republic of Korea

[105]Suranaree University of Technology, Nakhon Ratchasima, Thailand

[106]Technical University of Košice, Košice, Slovak Republic

[107]The Henryk Niewodniczanski Institute of Nuclear Physics, Polish Academy of Sciences, Cracow, Poland

[108]The University of Texas at Austin, Austin, Texas, USA

[109]Universidad Autónoma de Sinaloa, Culiacán, Mexico

[110]Universidade de São Paulo (USP), São Paulo, Brazil

[111]*Universidade Estadual de Campinas (UNICAMP), Campinas, Brazil*
[112]*Universidade Federal do ABC, Santo Andre, Brazil*
[113]*Universitatea Nationala de Stiinta si Tehnologie Politehnica Bucuresti, Bucharest, Romania*
[114]*University of Cape Town, Cape Town, South Africa*
[115]*University of Houston, Houston, Texas, USA*
[116]*University of Jyväskylä, Jyväskylä, Finland*
[117]*University of Kansas, Lawrence, Kansas, USA*
[118]*University of Liverpool, Liverpool, United Kingdom*
[119]*University of Science and Technology of China, Hefei, China*
[120]*University of South-Eastern Norway, Kongsberg, Norway*
[121]*University of Tennessee, Knoxville, Tennessee, USA*
[122]*University of the Witwatersrand, Johannesburg, South Africa*
[123]*University of Tokyo, Tokyo, Japan*
[124]*University of Tsukuba, Tsukuba, Japan*
[125]*Universität Münster, Institut für Kernphysik, Münster, Germany*
[126]*Université Clermont Auvergne, CNRS/IN2P3, LPC, Clermont-Ferrand, France*
[127]*Université de Lyon, CNRS/IN2P3, Institut de Physique des 2 Infinis de Lyon, Lyon, France*
[128]*Université de Strasbourg, CNRS, IPHC UMR 7178, F-67000 Strasbourg, France, Strasbourg, France*
[129]*Université Paris-Saclay, Centre d'Etudes de Saclay (CEA), IRFU,*
Départment de Physique Nucléaire (DPhN), Saclay, France
[130]*Université Paris-Saclay, CNRS/IN2P3, IJCLab, Orsay, France*
[131]*Università degli Studi di Foggia, Foggia, Italy*
[132]*Università del Piemonte Orientale, Vercelli, Italy*
[133]*Università di Brescia, Brescia, Italy*
[134]*Variable Energy Cyclotron Centre, Homi Bhabha National Institute, Kolkata, India*
[135]*Warsaw University of Technology, Warsaw, Poland*
[136]*Wayne State University, Detroit, Michigan, USA*
[137]*Yale University, New Haven, Connecticut, USA*
[138]*Yonsei University, Seoul, Republic of Korea*
[139]*Zentrum für Technologie und Transfer (ZTT), Worms, Germany*
[140]*Affiliated with an institute covered by a cooperation agreement with CERN*
[141]*Affiliated with an international laboratory covered by a cooperation agreement with CERN*

[†]Deceased.

[‡]Also at Max-Planck-Institut fur Physik, Munich, Germany.

[§]Also at Italian National Agency for New Technologies, Energy and Sustainable Economic Development (ENEA), Bologna, Italy.

[‖]Also at Dipartimento DET del Politecnico di Torino, Turin, Italy.

[¶]Also at An institution covered by a cooperation agreement with CERN.

[**]Also at Department of Applied Physics, Aligarh Muslim University, Aligarh, India.

[††]Also at Institute of Theoretical Physics, University of Wroclaw, Wroclaw, Poland.